Journal of the Physical Society of Japan
Vol. 66, No. 10, October, 1997, pp. 2973-2976



# Conductance of Carbon Nanotube Junctions in Magnetic Fields

Takeshi NAKANISHI and Tsuneya ANDO[1]

*The Institute of Physics and Chemical Research (RIKEN), 2–1 Hirosawa, Wako-shi, Saitama 351-01*
[1]*Institute for Solid State Physics, University of Tokyo, 7–22–1 Roppongi, Minato-ku, Tokyo 106*

(Received June 2, 1997)

The conductance of a junction connecting two carbon nanotubes of differing diameter is calculated in magnetic fields perpendicular to the tube axis. The relative importance of mixing between different valleys exhibits a characteristic change depending on the effective strength of the magnetic field in the two tubes. The conductance depends only on the component of the magnetic field in the direction of the pentagonal and heptagonal rings.

KEYWORDS: graphite, carbon nanotube, Fullerene tube, topological disorder, magnetoconductance, recursive Green's function technique, Landauer's formula, mesoscopic system

Recently Iijima[1] reported the observation of carbon nanotubes (CN's) consisting of graphite sheets rolled in cylindrical form. Defects in the hexagonal network responsible for the negative and positive curvature are heptagonal and pentagonal rings, respectively.[2] A junction with a pair of heptagonal and pentagonal rings which connects nanotubes of differing diameter has been observed by the transmission electron microscope.[3] The purpose of this work is to calculate the conductance of such junctions in the presence of magnetic fields perpendicular to the axis.

The band structure of single-shell CN's has been studied using a tight-binding method,[4-8] which shows that the CN's become a metal or a semiconductor depending on their structure, such as diameter and the helical arrangement. Because the distance between adjacent layers is much larger than the bond length between the nearest-neighbor sites within a layer, characteristic features of CN's are expected to be determined by those of a single-shell nanotube. In fact, a model calculation showed that effects of inter-shell interactions on electronic states are small.[9]

Recently, theoretical calculations on the transport of CN junctions were reported.[10-12] The tunneling conductance was calculated for a CN junction with a voltage drop,[10] and resonant tunneling conductance effects were shown for metal-metal and metal-semiconducting junctions. The conductance of junctions connecting two different metallic carbon nanotubes was calculated and shown to exhibit a universal power-law dependence on the ratio of their circumferences.[11,12] The mechanism leading to this intriguing result has not yet been fully understood.

In the presence of a magnetic field perpendicular to the tube axis, the band structure of CN is known to be strongly modified due to the formation of two-dimensional Landau states.[13,14] This gives rise to various peculiar effects on the electronic properties of CN's, including transport.[15,16] Therefore, the magnetic field is expected to have a strong influence on the conductance of junctions consisting of two CN's with differing circumferences.

We consider the junctions of two armchair CN's in magnetic fields, illustrated in Fig. 1(a). The axis of the two tubes with circumferences $L_5$ and $L_7$ ($L_5 > L_7$) is chosen in the $y$ direction. Both ends of the junction region contain a single pentagonal ring (denoted as R5) and a heptagonal ring (denoted as R7) present in the positive $z$ direction. The angle between the magnetic field with strength $H$ and the $z$ axis is denoted as $\theta_H$.

We use a tight-binding model with a nearest-neighbor hopping integral $\gamma_0$. A magnetic field is introduced through a Peierls phase factor.[17,18] The armchair CN is always metallic and has two bands in the vicinity of the Fermi energy crossing at $k_y = 2\pi/3a$ (K point) and $k_y = -2\pi/3a$ (K′ point) as is illustrated in Fig. 1(b).[4,6] The dispersion near the Fermi energy is approximately given by $\epsilon = \pm\gamma k$, where $k$ is the wave vector measured from the K and K′ point and $\gamma = \sqrt{3}a\gamma_0/2$ with $a$ being the lattice constant. Two channels denoted as K and K′ with positive velocity have the dispersion $\epsilon = +\gamma k$ and two with negative velocity have that of $\epsilon = -\gamma k$.

In Landauer's formula,[19] the conductance $G$ is defined by the sum of the total transmission probability for channels incident from left or right:

$$G = \frac{e^2}{\pi\hbar}\sum_{m,n}|t_{mn}|^2, \tag{1}$$

where $t_{mn}$ is the transmission coefficient for the incident channel $n$ on the left side and the outgoing channel $m$ in the right side. In the following, we shall confine ourselves to the case of $\varepsilon \sim 0$ and other cases will be discussed in a future publication. We have four combinations of channels $\{m,n\} = \{\mathbf{K},\mathbf{K}\}$, $\{\mathbf{K},\mathbf{K}'\}$, $\{\mathbf{K}',\mathbf{K}\}$ and $\{\mathbf{K}',\mathbf{K}'\}$.

The transmission coefficients are calculated numerically using a recursive Green's function technique.[20] The reflection coefficients $r_{mn}$ are calculated simultaneously and the unitarity of the scattering matrix is confirmed. The results show the desired symmetry properties $|t_{KK}| = |t_{K'K'}|$, $|t_{KK'}| = |t_{K'K}|$, $|r_{KK'}| = |r_{K'K}|$ and $|r_{KK}| = |r_{K'K'}|$.

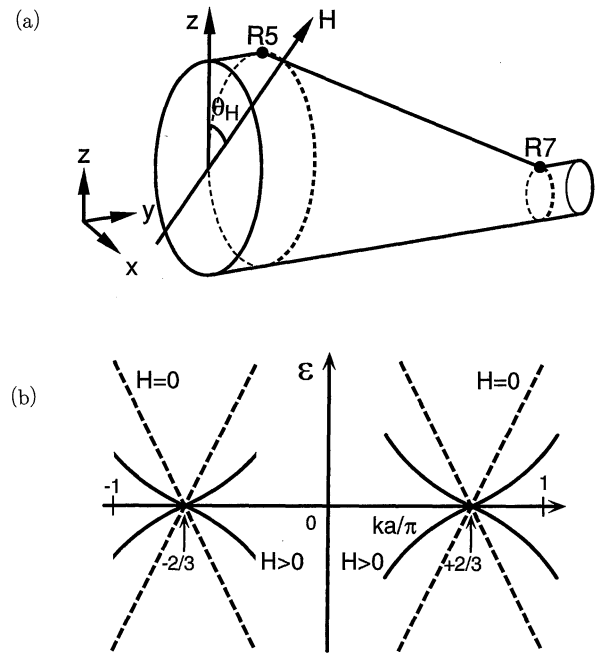


Fig. 1. (a) Illustration of a CN junction in a magnetic field perpendicular to the tube axis chosen in the $y$ direction. $R5$ and $R7$ indicate the position of the pentagonal and heptagonal rings, respectively. (b) Energy bands of an armchair nanotube in the vicinity of the Fermi level (the dashed lines indicate in the absence of a magnetic field and the solid lines are those of a strong magnetic field).

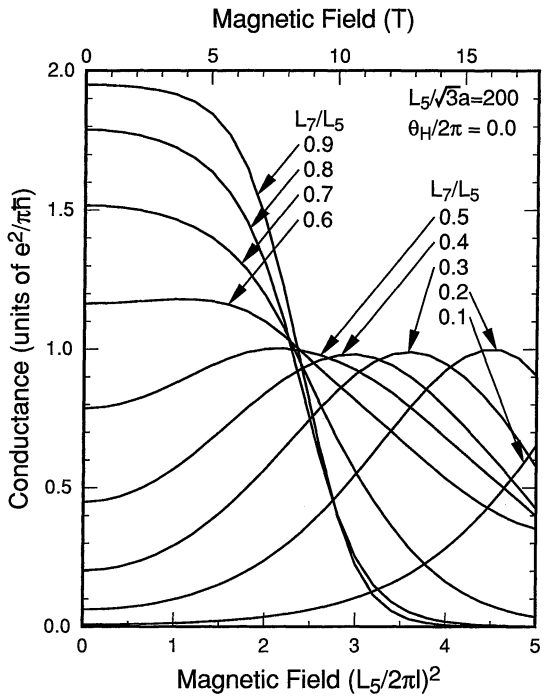


Fig. 2. Calculated conductance in units of $e^2/\pi\hbar$ as a function of the effective strength of a magnetic field in the thicker nanotube. The length of the junction is proportional to $L_5 - L_7$, where $L_5$ and $L_7$ are the circumference of the thicker and thinner CN, respectively.

In CN with circumference $L$, the effective strength of the magnetic field is characterized by $(L/2\pi l)^2$, which is the square of the ratio of the radius $L/2\pi$ and the magnetic length given by $l = \sqrt{c\hbar/eH}$.[13,14] We have two regimes: the weak-field regime $(L/2\pi l)^2 \ll 1$ and the strong-field regime $(L/2\pi l)^2 \gg 1$. In the latter case, Landau levels are formed at the position of the circumference in the positive and negative directions of the magnetic field and the extent of the Landau wave function is determined by $l$. In the former case the magnetic field can be treated as a small perturbation and the wave function is extended almost uniformly along the circumference.

We choose the large circumference $L_5/\sqrt{3}a = 200$ for the calculation in order to satisfy the condition $l \gg a$, which allows us to ignore the effects of the lattice. This corresponds to the diameter $L_5/\pi = 271$ Å with $a = 2.46$ Å, which is reasonable in comparison with the real CN whose diameter is usually between about 20 and 300 Å.[1,3] The present system is characterized by two circumferences $L_5$ and $L_7$ and we shall choose $(L_5/2\pi l)^2$ as a parameter to describe the effective strength of the magnetic field.

Figure 2 shows examples of calculated conductance as a function of the magnetic field for different $L_7$'s. In the case of a short junction $L_7 \sim L_5$, the conductance decreases with the increase of the magnetic-field strength. In the case of a long junction $L_7 \ll L_5$, for which the conductance at $H = 0$ is less than the unit of the conductance $e^2/\pi\hbar$, the conductance gradually increases, reaches a maximum and then decreases with the field.

Figure 3 shows transmission and reflection probabilities for a long (Fig. 3(a)) and short (Fig. 3(b)) junction. In the absence of a magnetic field, $t_{KK'} = t_{K'K} = r_{KK} = r_{K'K'} = 0$, i.e., transmissions are possible only within the same valley and reflections are allowed only between different valleys. In magnetic fields, transmissions between different valleys and reflections within the same valleys become allowed.

In Fig. 3(a) $(L_7/2\pi l)^2 = 0.36$ even for $(L_5/2\pi l)^2 = 4$, which means that the CN with circumference $L_7$ is still in a weak-field regime in this field. In Fig. 3(b), on the other hand, $(L_7/2\pi l)^2 \sim 2$ for $(L_5/2\pi l)^2 = 4$, which means both nanotubes are already in a strong field regime for $(L_5/2\pi l)^2 \sim 4$. Therefore, the mixing between the K and K′ valleys becomes appreciable for both transmission and reflection probabilities when the tube with a large circumference is in a high-field regime but that with a small circumference is still in a weak-field regime. In very high magnetic fields where the tube with a small circumference is also in a high-field regime, the reflection probabilities within the same valley become much larger than those between different valleys and the transmission probabilities between different valleys become much larger than those within the same valley. This behavior in the high-field regime is completely opposite to that in the absence of a magnetic field.

Figure 4 shows the dependence on the direction $\theta_H$ of the field. We notice that the conductance remains almost independent of the field when the field is parallel to the $x$-axis $(\theta_H = \pi/2)$. A remarkable result is that all the plots almost lie on the same line if being plotted as a function of $(L_5/2\pi l)^2 \cos\theta_H$. This means that the conductance is determined only by the magnetic-field component in the

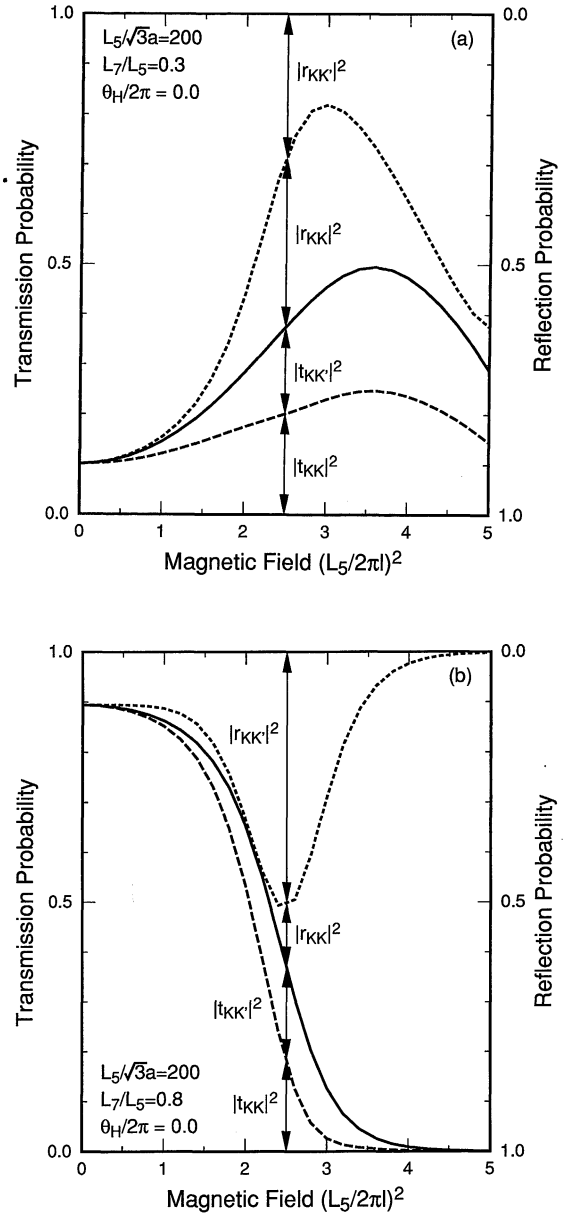


Fig. 3. Examples of calculated transmission and reflection probabilities as a function of the magnetic field for (a) long ($L_7/L_5 = 0.3$) and (b) short ($L_7/L_5 = 0.8$) junctions. The solid line represents the conductance $G$, which are the same as those given in Fig. 2. The dashed line represents the contribution of the transmission within the same valleys and the difference between the solid line and the dashed line that between different valleys. The difference between the dotted line and the solid line gives the reflection probabilities within the same valleys. The sum of all transmission and reflection probabilities becomes two because of the presence of two valleys.

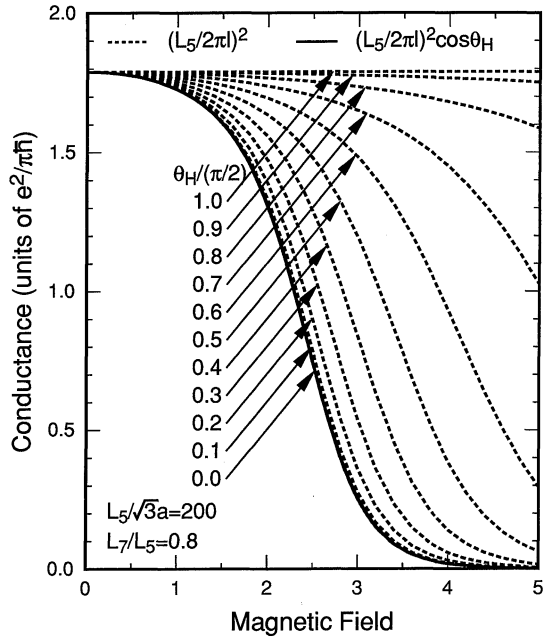


Fig. 4. Examples of the calculated conductance as a function of $(L_5/2\pi l)^2$ (dotted lines) and $(L_5/2\pi l)^2 \cos\theta_H$ (solid lines) for a junction in various field directions. The conductance for $\theta_H = 0$ is the same as that for $L_7/L_5 = 0.8$ in Fig. 2, where the magnetic field is applied parallel to the $z$ axis of Fig. 1(a). All lines are reduced to a single common curve if they are plotted as a function of $(L_5/2\pi l)^2 \cos\theta_H$.

$z$ direction where the pentagonal and heptagonal rings are present.

It is very difficult to provide an intuitive picture that explains the essential features of the results obtained. One simple model might be to replace the pentagonal and heptagonal rings by a scatterer with a short-range potential. This may explain the rapid decrease of the conductance as a function of the magnetic field for $L_7 \sim L_5$ shown in Fig. 2. In fact, the scattering from an impurity with a short-range potential leads to a similar decrease in the transmission probability.[15,16]

However, this model cannot explain the field-dependence for a longer junction $L_7/L_5 \lesssim 1/2$, as shown in Fig. 2. Furthermore, it contradicts the fact that the conductance is independent of the field for $\theta_H = \pi/2$, as shown in Fig. 4. In this case, two nanotubes forming a junction are already in the strong-field regime for $(L_5/2\pi l)^2 \sim 4$ and therefore, the amplitude of the wave function at the position of the topological defects is exponentially small for $\theta_H = \pi/2$. This should give rise to a considerable increase in the transmission probability instead of field-independent behavior.

The results presented here seem to suggest that mixing between valleys K and K′ in the vicinity of the topological defects is more important than direct scattering from them. In fact, the transmission and reflection probabilities between the valleys alter their features in a very interesting way, as demonstrated in Fig. 3. However, in order to reach full understanding of the scattering mechanism in such CN junctions, more extensive calculations should be performed for varieties of junctions with different structures.

In summary, we have studied the conductance of a junction connecting two armchair CN's of differing circumferences in magnetic fields perpendicular to the tube axis. The symmetry of transmission and reflection probabilities among the channels associated with K and K′ points of a graphite sheet, its characteristic change in the presence of a magnetic field, and a universal behavior in the dependence on the field direction have been demonstrated.

## Acknowledgments

This work was supported in part by a Grant-in-Aid for Scientific Research from the Ministry of Education, Science and Culture. Numerical calculations were performed in part on the FACOM VPP500 in the Supercomputer Center, Institute for Solid State Physics, University of Tokyo.

1) S. Iijima: Nature (London) **354** (1991) 56.
2) B. I. Dunlap: Phys. Rev. B **49** (1994) 5643.
3) S. Iijima, T. Ichihashi and Y. Ando: Nature (London) **356** (1992) 776.
4) R. Saito, M. Fujita, G. Dresselhaus and M. S. Dresselhaus: Phys. Rev. B **46** (1992) 1804.
5) J. W. Mintmire, B. I. Dunlap and C. T. White: Phys. Rev. Lett. **68** (1992) 631.
6) N. Hamada, S. Sawada and A. Oshiyama: Phys. Rev. Lett. **68** (1992) 1579.
7) K. Tanaka, K. Okahara, M. Okada and T. Yamabe: Chem. Phys. Lett. **191** (1992) 469.
8) M. S. Dresselhaus, G. Dresselhaus and R. Saito: Solid State Commun. **84** (1992) 201.
9) R. Saito, M. Fujita, G. Dresselhaus and M. S. Dresselhaus: Appl. Phys. Lett. **60** (1992) 2204.
10) R. Saito, G. Dresselhaus and M. S. Dresselhau: Phys. Rev. B **53** (1996) 2044.
11) R. Tamura and M. Tsukada: Solid State Commun. **101** (1997) 601.
12) R. Tamura and M. Tsukada: Phys. Rev. B **55** (1997) 4991.
13) H. Ajiki and T. Ando: J. Phys. Soc. Jpn. **62** (1993) 1255.
14) H. Ajiki and T. Ando: J. Phys. Soc. Jpn. **62** (1993) 2470.
15) T. Seri and T. Ando: J. Phys. Soc. Jpn. **66** (1997) 169.
16) T. Ando and T. Seri: J. Phys. Soc. Jpn. (in press).
17) H. Ajiki and T. Ando: J. Phys. Soc. Jpn. **65** (1996) 505.
18) R. Saito, G. Dresselhaus and M. S. Dresselhaus: Phys. Rev. B **50** (1994) 14698 [Erratum: **53** (1996) 10408].
19) R. Landauer: IBM J. Res. Dev. **1** (1957) 223; Philos. Mag. **21** (1970) 863.
20) T. Ando: Phys. Rev. B **44** (1991) 8017.